Continuum Mech. Thermodyn. (2019) 31:969–987
https://doi.org/10.1007/s00161-018-0698-7

ORIGINAL ARTICLE

**Massimo Cuomo**

# Continuum damage model for strain gradient materials with applications to 1D examples

Received: 7 January 2018 / Accepted: 18 July 2018 / Published online: 26 July 2018


**Abstract** In complex materials there exist different, often independent, mechanisms for the evolution of anelastic phenomena at the micro- and at the macroscale. Consequently, gradient plasticity has been introduced for a large variety of non-local materials. In a similar way, continuum damage has been extended to micromorphic and other non-local models, introducing internal damage variables and their gradient. In the paper is proposed a new continuum damage model for strain gradient materials characterized by two independent damage internal variables, each evolving with its own law. In this way, no additional field equation for the damage variable is needed. The model is intended to be used for metamaterials. Some important characteristics of the model are analysed with numerical analyses of a 1D example. In particular, the ability of the model to prevent strain localization is discussed.

**Keywords** Continuum damage · Strain gradient material · Non-local materials · Strain localization

## 1 Introduction

Continuum damage mechanics is largely employed for modelling the reduction of the mechanical performances due to the modifications of the internal structure of the material. Damage models are used for several phenomena, ranging from voids growth and coalescence to fatigue and fracture simulations. An overview of some applications can be found in [48]. The scale at which *continuum damage* occurs is usually the same at which strain is measured.

Advanced engineering materials present, on the other side, a complex microstructure, specifically designed in order to develop exotic properties, like selective wave absorption, tunable resonance, auxetic behaviour, etc. [5,9,63]. A large class of new materials, referred to with many different denominations, and that in this paper will generically be indicated as *metamaterials*, present a microstructure that can be considered with some approximation periodic, quasi-periodic or randomly periodic. Materials with inclusions of different phases and, especially, with a lattice microstructure are included among them. An overview of some recent advances in the design of metamaterials can be found in [51,56,57]. Homogenization procedures based on asymptotic expansion or other similar techniques are used for obtaining effective mechanical properties, (see for instance [13,14,25,38,45,58,65]. Unless the microscale is particularly small (of the order of less than 1 nm), continuum models are still applicable to the microstructure, so that equivalent properties for the continuum can be obtained. However, it has been shown that the Cauchy continuum model is not always applicable, rather micropolar, higher gradient, Cosserat or other non-local material models are more appropriate [18,24,45,66].

Communicated by Francesco dell'Isola.

M. Cuomo (✉)
Department of Civil Engineering and Architecture, University of Catania, Catania, Italy
E-mail: mcuomo@dica.unict.it

Most of the results of homogenization for metamaterials have been obtained in the elastic range, either linear or nonlinear. Applications of anelastic homogenization are known in several fields, like composites and lattice media [8,15,17,49], wave propagation [40], masonry [1,23], etc. In materials with microstructure, the resulting constitutive equations strongly depend on the nature of the microstructure [6], and in general it is necessary to distinguish between anelastic phenomena occurring at the microscale or at the macroscale. For instance in lattice materials buckling may occur in the microstructure, reducing its stiffness, or instability phenomena may interest the macroscale (similarly to what happens in space truss structures, where localized or extended buckling modes can arise). Buckling at the microscale is one of the inelastic mechanisms that characterize metallic foams and that causes localization of deformation. The response of metallic foams is quite different from standard materials: a ductile behaviour is observed in compression as opposed to a brittle response in tension, even if the basic material is a ductile metal. The presence of a microstructure induces the onset of localized deformations, even in a state of macroscopically homogeneous stress, that are not observed in standard continua [26,35,53,62].

For second gradient and micromorphic materials have been proposed several plastic models, with hardening and softening as well [31,34,68]. The link between gradient plasticity and non-local deformation models was established in [2], and later in [33] a systematic theory of generalized continua within the framework of gradient elasto-plasticity was exposed.

In first gradient theories, the onset of softening causes the loss of coerciveness of the tangent stiffness operator, so that an unstable material response is obtained and localization arises. Numerically, this leads to mesh dependency of the simulations. Similarly, the onset of continuum damage (usually denoted by $d$, and that in this paper will be indicated by $\omega_p$) induces a reduction of the stiffness and, consequently, of the bearing capacity of the material, with strain localization and mesh dependency that cannot be avoided remaining in the field of continuum first-order theories.

Gradient plasticity and damage have been proposed and deeply investigated since the last decade of the past century, for regularizing softening and damage [4,11,30,36,67]. In the earliest models, damage was associated to first gradient elasticity, and the gradient of the damage was added, used as a regularizing parameter [3,52,70].

Continuum damage models for non-local materials, although less common than plasticity models, have been introduced in a similar way to non-local plasticity, that is, adding an internal mechanism for microdamage, ruled by a local internal micromorphic variable [31,41]. Damage evolution is determined by conjugate forces, related to the local value of the damage variables and to its gradient. An additional differential equation is then obtained for damage compatibility. Non-local damage models have been mostly introduced for micromorphic materials. Placidi has proposed a damage model for strain gradient materials with one additional damage parameter, within a general formulation for strain gradient materials previously formulated [54,55,60]. The non-local damage model has been presented in the uniaxial case, proving the ability of the formulation to prevent localization and to sustain also concentrated actions. The relation between localization and the violation of ellipticity in generalized continua has been analysed in connection to some of the models proposed [7,27,28].

A plasticity model for strain gradient materials with softening was presented in [19]. Its main original contribution was to include in the plasticity model two different variables for macro- and microplastic deformations and for macro- and microhardening/softening, evolving independently according to specific flow rules, so that no additional differential equation was needed. With the aid of a localization analysis, it was found the rather surprising result that even in the case that both first and second plasticity present softening, plastic strains do not localize, rather a finite plastic band is obtained, thanks to the presence of strain gradients in the model.

In this paper is presented a damage model for strain gradient materials that uses different and independent variables for macro- and microdamage, similarly to the model already developed for non-local plasticity. The derivation will be obtained within a thermodynamic framework, introducing suitable functionals for the internal energy and for the rate of dissipation.

Specific objectives of the work are thus:

- to present a damage model for strain gradient materials that does not need the solution of additional differential equations;
- to analyse a simpler version of the model, in order to compare it with local damage models
- to study whether also in this case, similarly to what has been found with non-local softening plasticity models, the presence of strain gradients is able to avoid strain localization and consequently mesh dependency in the numerical simulations.

As it will be shown in the next sections, a rigorous localization analysis appears difficult to perform, since the stiffness of the system depends in a strong nonlinear way by the current state, so a general solution appears

difficult to obtain. The question will be analysed with the aid of numerical simulations of an uniaxial problem, in a static regime. The conclusions will not be, of course, general, but will yield useful indications for future investigations.

In Sect. 2, the model will be presented in a general setting. The general framework proposed in [16] will be used, where some useful information about the links of the model with traditional formulations using effective stresses and strains can be found. The model will be restricted to pure damage in Sect. 3. Then in Sect. 4 the model will be applied to a 1D example. A numerical analysis will then be performed, using isogeometric interpolation. The results of numerical tests will be discussed. Finally, some conclusions related to the stated objectives will be drawn.

## 2 Constitutive model of second gradient damage

### 2.1 State variables

The model is set within the limits of the linear theory of infinitesimal deformation. Most of the non-local models for damage proposed so far are restrained to this hypothesis. Higher gradient models have been extended to large deformation in the case of plasticity and damage [10,50,59,61], but they require a different treatment, of the type of the one presented in [21,22].

The domain occupied by the body will be denoted by $\Omega \subset \mathrm{R}^d$, with $d$ the dimension of the ambient space. A Cartesian reference frame $x^i$ will be used, and the displacement will be indicated by the vector function $\boldsymbol{u}(\boldsymbol{x}) \in \mathcal{V} : \Omega \to \mathrm{R}^d$ with $\mathcal{V} \subset \mathrm{H}^2(\Omega)$.

A set of state variables describes the evolution of the system: for a strain gradient material, the deformation is defined by the strain and by the strain gradient tensors:

- $\varepsilon \in \mathcal{D}$ macroscopic strain
- $\eta \in \mathcal{C}$ strain gradient

with

$$\varepsilon_{ij} = \frac{1}{2}\left(\frac{\partial u_i}{\partial x^j} + \frac{\partial u_j}{\partial x^i}\right) \qquad \eta_{ijk} = \frac{1}{2}\left(\frac{\partial^2 u_i}{\partial x^j \partial x^k} + \frac{\partial^2 u_j}{\partial x^i \partial x^k}\right). \tag{1}$$

$\mathcal{D}, \mathcal{C}$ are suitable functional spaces with the required regularity in order for the derivatives to be well defined. As usual, $\mathcal{D}$ is the space of the second-order tensors whose components are elements of $\mathrm{H}^1(\Omega)$, while $\mathcal{C}$ is the space of the third-order tensors whose components are elements of $\mathrm{L}^2(\Omega)$.

Additional internal variables are needed for the damage evolution. Damage, in general, is non-isotropic and unilateral. Typical example is the development of microfractures, that causes damage mostly in the direction normal to fracture, also causing a reduction of the shear stiffness. In consideration of the directional nature of damage, first gradient continuum damage models assume as damage internal variable a second-order tensor, whose contraction with the strain tensor defines the so-called effective strain. A similar approach appears to be necessary also in the case of non-local damage models. However the definition of a general third-order effective strain tensor requires the introduction of second-, third- and forth-order damage tensors, with very many components of difficult physical interpretation. As a matter of fact, most of the non-local damage models proposed so far are isotropic, that is they use a single scalar damage variable [32]. Therefore in this paper only isotropic damage is considered, characterised by two additional internal scalar variables for the damage evolution, one affecting the first gradient strain energy, the other affecting the second gradient strain energy:

$\omega_1 \in \mathcal{R}$ first gradient damage variable
$\omega_2 \in \mathcal{R}$ second gradient damage variable

Altogether the set of kinematic state variables will also be denoted by $\gamma = (\varepsilon, \eta, \omega_1, \omega_2)$. To each kinematic variable corresponds a mechanic counterpart, an element of the dual space, i.e. (a prime denotes the adjoint space)

$\sigma \in \mathcal{D}'$ stress
$\mu \in \mathcal{C}'$ hyperstress
$\zeta_1 \in \mathcal{R}$ damage driving force (released energy)
$\zeta_2 \in \mathcal{R}$ second gradient damge driving force

All the conjugated internal forces will be denoted by $\tau = (\sigma, \mu, \zeta_1, \zeta_2)$. In the paper, rates are indicated by a superposed dot. The duality product of the conjugated variables in the relevant spaces generates the bilinear form of the internal virtual power, indicated by brackets:

$$P_{vi} = \underbrace{\langle \sigma, \dot{\varepsilon} \rangle_{\mathcal{D}} + \langle \mu, \dot{\eta} \rangle_{\mathcal{C}}}_{\text{Mechanical Power}} + \zeta_1 \dot{\omega_1} + \zeta_2 \dot{\omega_2} \tag{2}$$

For the virtual power equality, the first two addends are recognized to be the mechanical power, and the terms not underbraced in Eq. (2) are then globally null, since for any closed system the power of the internal variables is zero. Each kinematic variable is decomposed in a reversible and an irreversible components, the first responsible for energy storage and the second associated to dissipated power. For the infinitesimal kinematics considered in this work, an additive decomposition is obtained. For a general elastic-plastic damaging material, both the strains and the damage variables are decomposed in this way:

$$\varepsilon = \varepsilon_e + \varepsilon_p \tag{3}$$
$$\eta = \eta_e + \eta_p \tag{4}$$
$$\omega_1 = 0 = \omega_{1e} + \omega_{1p} \tag{5}$$
$$\omega_2 = 0 = \omega_{2e} + \omega_{2p} \tag{6}$$

Notice that the damage variables are globally zero, so that the duality products in Eq. (2) vanish. However, their elastic and plastic components are individually different from zero. In order to complete the material model, following the framework of the Generalised Standard Material Model (GSMM) [44], it is necessary to define the form of the internal energy functional and of the rate of dissipation functional, that depend on the local values of the kinematic variables.

## 2.2 Thermodynamic consistency

According to the GSMM, the specific internal energy $e$ is a potential of the reversible parts of the state variables only, i.e.

$$e = e(\varepsilon_e, \eta_e, \omega_{1e}, \omega_{2e}, s) \tag{7}$$

where $s$ is the specific entropy.

Indicating with $r$ the specific heat production in a reversible process, with $\boldsymbol{q}$ the heat flux, the first principle of thermodynamics in the present setting reads

$$\rho\, \dot{e} = \sigma \cdot \dot{\varepsilon} + \mu \cdot \dot{\eta} + r - \mathrm{div}\boldsymbol{q} \tag{8}$$

Here and in the following a dot denotes the scalar product between tensors of any order.

The second principle of thermodynamics in the form due to Clausius and Duhem, states that:

$$\int_V \dot{s}\, \mathrm{d}V \geq \int_V \frac{r}{T}\, \mathrm{d}V - \int_{\partial V} \frac{\boldsymbol{q}}{T} \mathrm{d}S \tag{9}$$

where the sum of the last two integrals is the total heat production $Q/T$. The local form of the second law is then

$$\dot{s} \geq \frac{r}{T} - \mathrm{div}\frac{\boldsymbol{q}}{T} \tag{10}$$

The last term is the so-called "entropy flux". Eliminating the heat radiation via the first principle, it is obtained the local form of the Clausius–Duhem inequality:

$$\sigma \cdot \dot{\varepsilon} + \mu \cdot \dot{\eta} - \rho\, (\dot{e} - T\dot{s}) - \boldsymbol{q} \cdot \frac{\nabla T}{T} \geq 0 \tag{11}$$

Using the elastic constitutive equations (that derive from Coleman–Noll procedure)

$$\begin{array}{cc} \sigma = \rho\, \partial_{\varepsilon_e} e & \mu = \rho\, \partial_{\eta_e} e \\ \zeta_1 = \rho\, \partial_{\omega_{1e}} e & \zeta_2 = \rho\, \partial_{\omega_{2e}} e \\ T = \partial_s e & \end{array} \tag{12}$$

the Clausius–Duhem inequality (11) reduces to

$$\rho T \dot{s}_p + \sigma \cdot \varepsilon_p + \mu \cdot \eta_p + \zeta_1 \, \omega_{1p} + \zeta_2 \, \omega_{2p} - \frac{\boldsymbol{q}}{T} \cdot \mathrm{grad} T \geq 0 \tag{13}$$

that gives the total dissipation rate. The term $\dot{s}_p$ is related to Clausius uncompensated heat [29,69].

The mechanical rate of dissipation $d$ is thus a functional of the irreversible components of the kinematic variables,

$$d = d(\varepsilon_p, \eta_p, \omega_{1p}, \omega_{2p}). \tag{14}$$

## 2.3 Constitutive assumptions

### *2.3.1 Strain energy*

Since isothermal processes only will be considered, only the strain energy $\phi$ needs to be specified for defining the internal energy. It is taken as a generalization of the strain energy used for strain gradient materials, that is a sum of two uncoupled contributions of the first and second gradient strains:

$$e(\varepsilon_e, \eta_e, \omega_{1e}, \omega_{2e}) = \frac{1}{2}\boldsymbol{E}(1+\omega_{1e})^{n_1}\varepsilon_e \cdot \varepsilon_e + \frac{1}{2}\boldsymbol{G}(1+\omega_{2e})^{n_2}\eta_e \cdot \eta_e + \mathcal{U}_1(\omega_{1e}) + \mathcal{U}_2(\omega_{2e}) \tag{15}$$

Since the damage variables are negative (as will appear from the evolution equations of the dissipation), they cause a reduction of the elastic stiffness. The functions $\mathcal{U}_i$ are indicator functions of the set $(-1, 0)$, and they enforce the damage variables to never become smaller than $-1$: indeed, in this case zero stiffness is attained. However, the upper limit is never violated, since $\omega_{ie} \leq 0$, $i = 1, 2$, and according to the rate equation used for the damage evolution the lower limit also can never be attained. However, the presence of the constraint is useful in numerical implementations.

$\boldsymbol{E}$, $\boldsymbol{G}$ are forth- and sixth-order positive definite tensors. The scalars $n_1, n_2$ are positive exponents strictly greater than 1 that rule the intensity of damage. The elastic constitutive equation are then

$$\begin{aligned}
\sigma &= \boldsymbol{E}\,\varepsilon_e(1+\omega_{1e})^{n_1} \\
\mu &= \boldsymbol{G}\,\eta_e(1+\omega_{2e})^{n_2} \\
\zeta_1 &= \frac{n_1}{2}\boldsymbol{E}\,\varepsilon_e \cdot \varepsilon_e(1+\omega_{1e})^{n_1-1} \\
\zeta_2 &= \frac{n_2}{2}\boldsymbol{G}\,\eta_e \cdot \eta_e(1+\omega_{2e})^{n_2-1}
\end{aligned} \tag{16}$$

Notice that the present model rules out the possibility to set the exponent of the damage law to 1, as instead is a common choice in other damage models not based on the thermodynamic framework presented here. Also, it has been raised the possibility that different internal mechanisms act on the macro- and on the microscales. For instance, in [54,55] it has been postulated that damage at the macroscale may induce some hardening process in the microscale. Although the tensors $\boldsymbol{E}$, $\boldsymbol{G}$ are positive definite, and $n_1, n_2$ are positive, the strain energy functional (15) is not convex. This can be seen evaluating the tangent stiffness operator $\boldsymbol{S}_t$:

$$\begin{pmatrix} \dot{\sigma} \\ \dot{\zeta}_1 \\ \dot{\mu} \\ \dot{\zeta}_2 \end{pmatrix} = \left(\begin{array}{c|c} \boldsymbol{E}_t & \hat{\boldsymbol{0}} \\ \hline \hat{\boldsymbol{0}} & \boldsymbol{G}_t \end{array}\right) \begin{pmatrix} \dot{\varepsilon}_e \\ \dot{\omega}_{1e} \\ \dot{\eta}_e \\ \dot{\omega}_{2e} \end{pmatrix} \tag{17}$$

where $\boldsymbol{0}$ is the zero tensor in $\mathcal{D} \times \mathcal{C}$ and

$$\begin{aligned}
\boldsymbol{E}_t &= \begin{pmatrix} \boldsymbol{E}\,(1+\omega_{1e})^{n_1} & n_1\boldsymbol{E}\,\varepsilon_e(1+\omega_{1e})^{n_1-1} \\ n_1\boldsymbol{E}\,\varepsilon_e(1+\omega_{1e})^{n_1-1} & \frac{n_1(n_1-1)}{2}\boldsymbol{E}\,\varepsilon_e \cdot \varepsilon_e(1+\omega_{1e})^{n_1-2} \end{pmatrix} \\
\boldsymbol{G}_t &= \begin{pmatrix} \boldsymbol{G}\,(1+\omega_{2e})^{n_2} & n_2\boldsymbol{G}\,\eta_e(1+\omega_{2e})^{n_2-1} \\ n_2\boldsymbol{G}\,\eta_e(1+\omega_{2e})^{n_2-1} & \frac{n_2(n_2-1)}{2}\boldsymbol{G}\,\eta_e \cdot \eta_e(1+\omega_{2e})^{n_2-2} \end{pmatrix}
\end{aligned} \tag{18}$$

Since the operator is uncoupled, the damage variables can be easily condensed, to obtain:

$$\begin{aligned}
&\begin{pmatrix} \hat{\boldsymbol{E}}_t & \mathbf{0} \\ \mathbf{0} & \hat{\boldsymbol{G}}_t \end{pmatrix} \begin{pmatrix} \dot{\varepsilon}_e \\ \dot{\eta}_e \end{pmatrix} = \begin{pmatrix} \dot{\sigma} - \frac{2}{n_1-1}\boldsymbol{E}\varepsilon_e(1+\omega_{1e})\frac{\dot{\zeta}_1}{\boldsymbol{E}\varepsilon_e\cdot\varepsilon_e} \\ \dot{\mu} - \frac{2}{n_2-1}\boldsymbol{G}\eta_e(1+\omega_{2e})\frac{\dot{\zeta}_2}{\boldsymbol{G}\eta_e\cdot\eta_e} \end{pmatrix} \\
&\hat{\boldsymbol{E}}_t = \boldsymbol{E}\,(1+\omega_{1e})^{n_1} - \frac{1}{\boldsymbol{E}\varepsilon_e\cdot\varepsilon_e}\frac{2n_1}{n_1-1}\boldsymbol{E}\,\varepsilon_e\otimes\boldsymbol{E}\varepsilon_e(1+\omega_{1e})^{n_1} \\
&\hat{\boldsymbol{G}}_t = \boldsymbol{G}\,(1+\omega_{2e})^{n_2} - \frac{1}{\boldsymbol{G}\eta_e\cdot\eta_e}\frac{2n_2}{n_2-1}\boldsymbol{G}\,\eta_e\otimes\boldsymbol{G}\eta_e(1+\omega_{2e})^{n_2}
\end{aligned} \tag{19}$$

For convexity, the tangent stiffness operator $\hat{\boldsymbol{S}}_t$, given by the matrix operator at the right-hand side of Eq. (19), must be positive definite, i.e. it must be

$$\hat{\boldsymbol{S}}_t\,\nu\cdot\nu > 0 \qquad \forall\nu\in\mathcal{D}\times\mathcal{C} \tag{20}$$

which implies

$$\begin{aligned}
\boldsymbol{E}\,\bar{\varepsilon}\cdot\bar{\varepsilon}\boldsymbol{E}\varepsilon_e\cdot\varepsilon_e &> \frac{2n_1}{n_1-1}\boldsymbol{E}\varepsilon_e\cdot\bar{\varepsilon}\boldsymbol{E}\varepsilon_e\cdot\bar{\varepsilon} \qquad \forall\bar{\varepsilon}\in\mathcal{D} \\
\boldsymbol{G}\,\bar{\eta}\cdot\bar{\eta}\boldsymbol{E}\eta_e\cdot\eta_e &> \frac{2n_21}{n_2-1}\boldsymbol{G}\eta_e\cdot\bar{\eta}\boldsymbol{E}\eta_e\cdot\bar{\eta} \qquad \forall\bar{\eta}\in\mathcal{C}.
\end{aligned} \tag{21}$$

Since $n_1 > 1, n_2 > 1$, the inequalities in Eq. (21) are clearly not true if one takes, for instance, $\bar{\varepsilon} = \varepsilon_e$, $\bar{\eta} = \eta_e$.

The constitutive relations (16) can be inverted (provided $n_1 > 1, n_2 > 1$) to yield:

$$\begin{aligned}
\varepsilon_e &= \boldsymbol{E}^{-1}\sigma\left(\frac{2}{n_1}\frac{\zeta_1}{\boldsymbol{E}^{-1}\sigma\cdot\sigma}\right)^{\frac{n_1}{1+n_1}} \\
\omega_{1e} &= -1+\left(\frac{2}{n_1}\frac{\zeta_1}{\boldsymbol{E}^{-1}\sigma\cdot\sigma}\right)^{-\frac{1}{1+n_1}} \\
\eta_e &= \boldsymbol{G}^{-1}\mu\left(\frac{2}{n_2}\frac{\zeta_2}{\boldsymbol{G}^{-1}\mu\cdot\mu}\right)^{\frac{n_2}{1+n_2}} \\
\omega_{2e} &= -1+\left(\frac{2}{n_2}\frac{\zeta_2}{\boldsymbol{G}^{-1}\mu\cdot\mu}\right)^{-\frac{1}{1+n_2}}
\end{aligned} \tag{22}$$

In (15), it has been assumed that the first and second gradient contributions are uncoupled, following a common hypothesis in strain gradient materials [37]. A more general assumption would be to consider a coupling (fifth order) tensor. An additional damage variable, say $\omega_{12}$, would then be needed in the model. However the difficulty for interpreting the elastic coefficients in this case suggests to avoid this case. Notice, however, that in the post-elastic regime the tangent stiffness operator presents in any case coupling between first and second gradient terms, as will be shown soon.

### *2.3.2 Dissipation functional*

Following the procedure outlined in [16] the rate of dissipation functional is introduced in an axiomatic way. The form assumed for the functional guarantees that an elastic nucleus exists, and that an inviscid dissipation model is obtained (the latter property follows from assuming that the dissipation is an homogeneous function of degree 1). Accordingly, the mechanical dissipation $d$, function of the irreversible components of the kinematic variables, is assumed to possess the following properties:

- $d = d(\dot{\varepsilon}_p, \dot{\eta}_p, \dot{\omega}_{1p}, \dot{\omega}_{2p}) : \mathcal{D}\times\mathcal{C}\times\mathcal{R}\times\mathcal{R} \to \mathrm{R}\cup+\infty : \begin{cases} d(0) = 0 \\ d(\dot{\gamma}_p) \geq 0 \,\text{otherwise} \end{cases}$
- $d$ is convex, proper and sublinear
- $d$ is such that the conjugated (static) variables belong to the subdifferential of $d$ at the point which represents the state of the system.

The condition that the dissipation functional be sublinear means that it must be subadditive and positively homogeneous of degree one. In this case an inviscid model, of damage and plasticity is obtained, see [20,39] for details. The last property guarantees the fulfilment of the reduced dissipation inequality, infact, since

$$\tau \in \partial_{\dot{\gamma}_p} d \Leftrightarrow \left\{\tau \,:\, \tau \cdot \left(\dot{\tilde{\gamma}}_p - \dot{\gamma}_p\right) \leq d(\dot{\tilde{\gamma}}_p) - d(\dot{\gamma}_p)\ \forall \dot{\tilde{\gamma}}_p\right\} \tag{23}$$

Taking $\dot{\tilde{\gamma}}_p = 0$ it follows immediately that $\tau \cdot \dot{\gamma}_p \geq d(\dot{\gamma}_p) \geq 0$ Therefore the mechanical dissipation is always nonnegative.

The closed convex set $K = \partial_{\dot{\gamma}_p} d\big|_0$ is the generalised elastic domain in the space of the conjugated thermodynamic forces, since all admissible internal forces obtained as subdifferential of the dissipation function belong to it [16,20]:

$$(\sigma, \mu, \zeta_1, \zeta_2) \in \partial d(\dot{\varepsilon}_p, \dot{\eta}_p, \dot{\omega}_{1p}, \dot{\omega}_{2p}) \subset \partial d(0) = K \tag{24}$$

The set of the admissible internal forces $K$, according to the hypotheses made for the dissipation, is convex and contains the origin. From the implication

$$\tau \in K = \partial d(0) \Leftrightarrow \tau \cdot \dot{\gamma}_p \leq d(\gamma_p)\ \forall \dot{\gamma}_p \tag{25}$$

it follows that the maximum dissipation principle is satisfied, that is

$$d(\dot{\gamma}_p) = \underset{\tau \in K}{sup} \tau \cdot \dot{\gamma}_p \tag{26}$$

From the latter statement it is seen that the dissipation functional is the support function of the convex set $K$, that will be indicated by the notation "supp $K$". Also, from the convexity of $K$, Drucker's stability principle holds. From a standard result of convex analysis the conjugated dissipation functional $d^c(\tau)$ is the Fenchel's transformation of $d$,

$$d(\gamma_p) = \mathrm{supp} K \Leftrightarrow d^c(\tau) = \mathrm{ind} K \tag{27}$$

where $\mathrm{ind} K$ denotes the indicator function of the set $K$, defined as:

$$\mathrm{ind} K = \begin{cases} 0 & \text{if } \tau \in K \\ +\infty & \text{otherwise} \end{cases} \tag{28}$$

The two conjugated dissipation functionals obey Fenchel's equality:

$$d(\dot{\gamma}_p) + d^c(\tau) = \tau \cdot \dot{\gamma}_p \Leftrightarrow \tau \in \partial d(\dot{\gamma}_p)\,,\ \dot{\gamma}_p \in \partial d^c(\tau) \tag{29}$$

The second implication is the flow rule for the anelastic kinematic variables

$$\dot{\gamma}_p \in \partial \mathrm{ind} K \tag{30}$$

that is, the rate of the anelastic internal variables must belong to the outward cone to the elastic domain in the point $\tau$

$$\gamma_p \in \mathcal{N}_K|_\tau\,, \tag{31}$$

the cone is empty if $\tau \in \overset{\circ}{K}$.

If the boundary of the convex domain of the admissible internal forces $K$ is defined by a suitable continuous function $g(\tau)$,

$$K = \{\tau \,:\, g(\sigma, \mu, \zeta_1, \zeta_2) \leq 0\} \tag{32}$$

the flow rule for the anelastic strain rates can be expressed as:

$$\begin{aligned} \dot{\varepsilon}_p &= \lambda\, \partial_\sigma g(\tau) \quad \dot{\eta}_p = \lambda\, \partial_\mu g(\tau) \\ \dot{\omega}_{1p} &= \lambda\, \partial_{\zeta_1} g(\tau) \quad \dot{\omega}_{2p} = \lambda\, \partial_{\zeta_2} g(\tau) \\ \lambda &\geq 0,\ g(\tau) \leq 0 \quad \lambda g(\tau) = 0 \end{aligned} \tag{33}$$

The last condition is a statement of the Kuhn–Tucker alternative.

The model is completed by the choice of the yield function $g(\tau)$. In general, the function $g$ does not need to be smooth, and although it is possible to use different yield functions for the stress and for the hyperstress, full coupling is included in the most general form. From the consistency condition

$$\dot{g} = \nabla_\sigma g \cdot \dot{\sigma} + \nabla_\mu g \cdot \dot{\mu} + \nabla_{\zeta_1} g\, \dot{\zeta}_1 + \nabla_{\zeta_2} g\, \dot{\zeta}_2 = 0 \tag{34}$$

using rate equations (17) and flow rule (33), it is possible to obtain the multiplier $\lambda$:

$$\begin{aligned}
\lambda &= \frac{1}{D_n}\left(\boldsymbol{E}(1+\omega_{1e})^{n_1}\left(\nabla_\sigma g + n_1\varepsilon_e\frac{\nabla_{\zeta_1} g}{1+\omega_{1e}}\right) + \boldsymbol{G}(1+\omega_{2e})^{n_2}\left(\nabla_\mu g + n_2\eta_e\frac{\nabla_{\zeta_2} g}{1+\omega_{2e}}\right)\right)\\
D_n &= (1+\omega_{1e})^{n_1}\left(\boldsymbol{E}\nabla_\sigma g\cdot\nabla_\sigma g + 2n_1\boldsymbol{E}\nabla_\sigma g\cdot\varepsilon_e\frac{\nabla_{\zeta_1} g}{1+\omega_{1e}} + \frac{n_1(n_1-1)}{2}\boldsymbol{E}\varepsilon_e\cdot\varepsilon_e\frac{\left(\nabla_{\zeta_1} g\right)^2}{(1+\omega_{1e})^2}\right)\\
&\quad +(1+\omega_{2e})^{n_2}\left(\boldsymbol{G}\nabla_\mu g\cdot\nabla_\mu g + 2n_2\boldsymbol{G}\nabla_\mu g\cdot\eta_e\frac{\nabla_{\zeta_2} g}{1+\omega_{2e}} + \frac{n_2(n_2-1)}{2}\boldsymbol{G}\eta_e\cdot\eta_e\frac{\left(\nabla_{\zeta_2} g\right)^2}{(1+\omega_{2e})^2}\right)
\end{aligned} \tag{35}$$

The tangent stiffness operator for anelastic evolution is thus:

$$\begin{aligned}
&\begin{pmatrix}\dot\sigma\\ \dot\mu\end{pmatrix} = \begin{pmatrix}(1+\omega_{1e})^{n_1}\left(\boldsymbol{E}-\boldsymbol{H}_1\otimes\boldsymbol{H}_1\frac{(1+\omega_{1e})^{n_1}}{D_n}\right) & -(1+\omega_{1e})^{n_1}\boldsymbol{H}_1\otimes\boldsymbol{H}_2\frac{(1+\omega_{2e})^{n_2}}{D_n}\\ -(1+\omega_{1e})^{n_1}\boldsymbol{H}_1\otimes\boldsymbol{H}_2\frac{(1+\omega_{2e})^{n_2}}{D_n} & (1+\omega_{2e})^{n_2}\left(\boldsymbol{G}-\boldsymbol{H}_2\otimes\boldsymbol{H}_2\frac{(1+\omega_{2e})^{n_2}}{D_n}\right)\end{pmatrix}\begin{pmatrix}\dot\varepsilon\\ \dot\eta\end{pmatrix}\\
&\boldsymbol{H}_1 = \boldsymbol{E}\left(\nabla_\sigma g + n_1\varepsilon_e\frac{\nabla_{\zeta_1} g}{1+\omega_{1e}}\right)\qquad \boldsymbol{H}_2 = \boldsymbol{G}\left(\nabla_\mu g + n_2\eta_e\frac{\nabla_{\zeta_2} g}{1+\omega_{2e}}\right)
\end{aligned} \tag{36}$$

As observed previously, the tangent stiffness presents coupling between first and second gradient deformation, even though the elastic tensor was assumed uncoupled. That is, any anelastic phenomena occurring at any one scale affects the overall material properties. The tensors $\boldsymbol{H}_1$, $\boldsymbol{H}_2$ rule the degradation of the material stiffness. Notice that in the present model the evolution of the internal variables and of the internal forces are obtained solving a *local* nonlinear problem, since all the variables are defined in the same point (the Gauss point in a numerical implementation). It has to be noticed that $\dot\eta_p$ is not the gradient of $\dot\varepsilon_p$, since it is obtained independently from the flow rule, and that the two damage variables evolve independently, without any need for additional equations.

The model introduced so far couples damage with plasticity (hardening has not been considered for simplicity, but can be easily added), that is, damage occurs together with the development of irreversible strains. In the next section the model will be restricted to the case of damage only.

## 3 Pure damage model

It is assumed that the dissipation depends only on the internal variables $\omega_{1p}, \omega_{2p}$. Therefore the strain and the gradient of strain tensors are totally elastic, $\varepsilon = \varepsilon_e,\ \eta = \eta_e$. The elastic constitutive relations are taken in the same form as in Eq. (16). From result (26), it follows that the dissipation rate functional is the support function of the domain

$$K = \{\zeta_1, \zeta_2 : g(\zeta_1, \zeta_2) \le 0\}\,. \tag{37}$$

that is, the elastic domain depends only on the damage internal forces. A linear form for the function $g$ will be used, that is:

$$g(\zeta_1, \zeta_2) = (1-c)\,\zeta_1 + c\,\zeta_2 - \zeta_0 \le 0 \tag{38}$$

The parameter $c$ rules the relative weight of the two internal damage forces. In order to get an insight in the model, and to highlight the effect of the exponents $n_1, n_2$, in Fig. 1 is shown the response to an uniaxial load for a first gradient material, as a function of $n_1$. The stress approaches zero asymptotically, and the closer the exponent to 1 the sharper is the stiffness reduction due to damage, while for values of $n_1$ larger than about 10 a limit behaviour is reached. A linear decreasing branch of the stress strain curve is not possible with this model.

Tangent stiffness (36) becomes in this case:

$$\begin{aligned}
&\begin{pmatrix}\boldsymbol{E}_d - n_1^2\boldsymbol{E}_d\varepsilon_e\otimes\boldsymbol{E}_d\varepsilon_e\left(\frac{1-c}{1+\omega_{1e}}\right)^2\frac{1}{D_n} & -n_1n_2\boldsymbol{E}_d\varepsilon_e\otimes\boldsymbol{G}_d\eta_e\frac{1-c}{1+\omega_{1e}}\frac{c}{1+\omega_{2e}}\frac{1}{D_n}\\ -n_1n_2\boldsymbol{E}_d\varepsilon_e\otimes\boldsymbol{G}_d\eta_e\frac{1-c}{1+\omega_{1e}}\frac{c}{1+\omega_{2e}}\frac{1}{D_n} & \boldsymbol{G}_d - n_2^2\boldsymbol{G}_d\eta_e\otimes\boldsymbol{G}_d\eta_e\left(\frac{c}{1+\omega_{2e}}\right)^2\frac{1}{D_n}\end{pmatrix}\\
&\boldsymbol{E}_d = \boldsymbol{E}(1+\omega_{1e})^{n_1}\qquad \boldsymbol{G}_d = \boldsymbol{G}(1+\omega_{2e})^{n_2}\\
&D_n = \frac{n_1(n_1-1)}{2}\boldsymbol{E}\varepsilon_e\otimes\varepsilon_e(1-c)^2(1+\omega_{1e})^{n_1-2} + \frac{n_2(n_2-1)}{2}\boldsymbol{G}\eta_e\otimes\eta_e c^2(1+\omega_{2e})^{n_2-2}
\end{aligned} \tag{39}$$

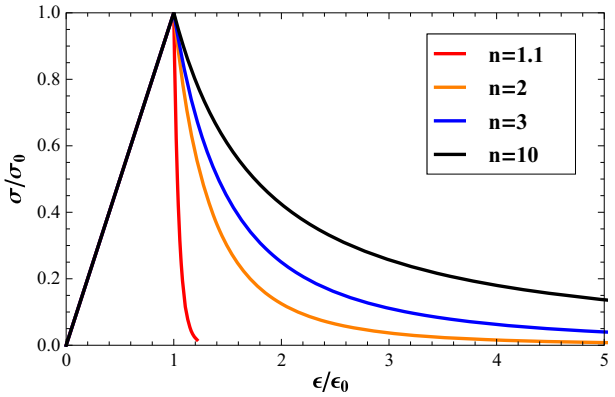


**Fig. 1** Damage model for a first gradient material. Uniaxial stress/strain response. $\sigma_0 = E\sqrt{\frac{2}{n_1}\frac{\zeta_0}{E}}$, $\varepsilon_0 = \frac{\sigma_0}{E}$

The evolution laws for the damage variables are

$$\omega_{1e} = -\omega_{1p} = -\lambda\,(1-c) \qquad \omega_{2e} = -\omega_{2p} = -\lambda\,c \tag{40}$$

The multiplier $\lambda$ is obtained, simultaneously to the stresses and damage forces, solving the local inverse constitutive relations. In the numerical implementation the rate problem is converted in incremental form, and the local problem to be solved becomes:

$$\begin{gathered}
\varepsilon_e(\sigma,\zeta_1) = \varepsilon \\
\eta_e(\mu,\zeta_2) = \eta \\
\omega_{1e}(\sigma,\zeta_1) + \lambda\,(1-c) + \omega_{1p}^0 = 0 \\
\omega_{2e}(\mu,\zeta_2) + \lambda\,c + \omega_{2p}^0 = 0 \\
\zeta_0 - (1-c)\,\zeta_1 - c\,\zeta_2 = 0
\end{gathered} \tag{41}$$

where the elastic kinematic variables are obtained from the inverse elastic constitutive relations (22), and $\omega_{1p}^0$, $\omega_{2p}^0$ are the historic values of the damage variables.

## 4 Uniaxial exemplification

The damage model described in Sect. 3 is applied to the uniaxial extension of a bar built in at one end and subjected to an imposed displacement at the free end (Fig. 2). This is a classical problem used for analysing strain localization, [46,64]. Indeed, for a first gradient material model with damage, an homogeneous stress state is obtained, so that in order to initialize damage it is necessary to introduce in the bar a region of length $a < L$ where a slightly smaller resistance is considered. Damage concentrates in the weaker region, while all the rest of the bar unloads elastically. As $a \to 0$ damage localizes in the narrow weak band, and in the limit no dissipation is obtained, since a continuum damage model is not able to simulate a process where energy is dissipated on a surface. A numerical simulation would present mesh dependency, similar to the results shown in Fig. 3. Snap back is predicted by the damage model, so that careful numerical techniques have to be adopted. In a strain gradient model, however, the stress field is not homogeneous. In [19] it was found in the context of softening plasticity that the presence of higher gradient strains was able to avoid strain localization and thus to allow the use of a continuous plasticity model for the simulation of the test.

Since the bar is built in, it is considered that both the displacement $u$ and its first derivative are zero at the first end of the bar, while the hyperstress $\mu$ is zero at the free end, where the displacement is imposed. An uniaxial particularization of the constitutive model is used, with uncoupled elastic stiffness. $E$ is the Young modulus, while $G = \ell^2 E$, with $\ell$ an internal length. The equilibrium equation of the bar, given by

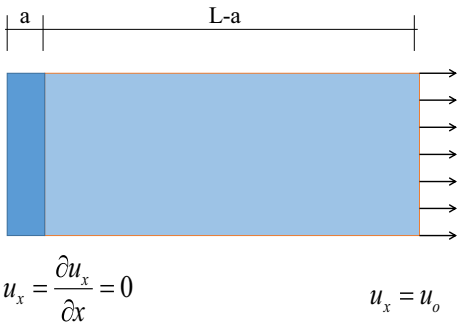


**Fig. 2** Uniaxial bar subjected to extension

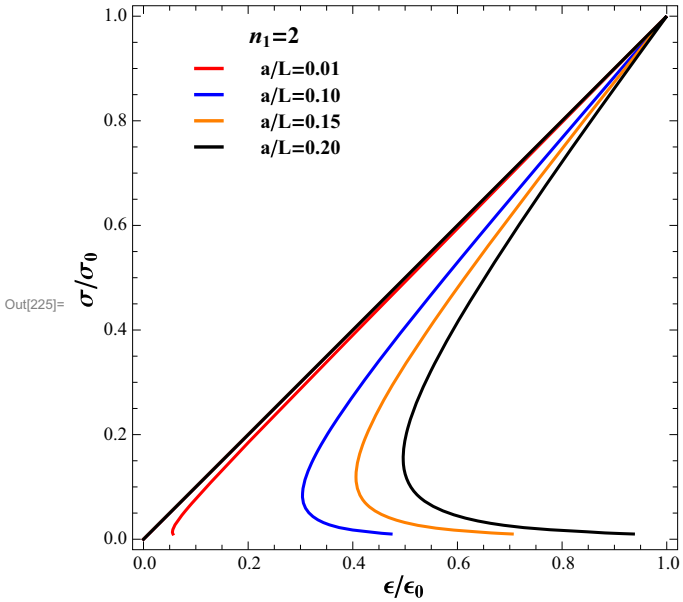


**Fig. 3** Damage model for a first gradient material. Uniaxial deformation of a bar with a weak segment of length $a$. $N_0 = EA\sqrt{\frac{2}{n_1}\frac{\zeta_0}{E}}$, $u_0 = \frac{N_0 L}{EA}$

$$EA\left(-\frac{\mathrm{d}^2u}{\mathrm{d}x^2} + \ell^2\frac{\mathrm{d}^4u}{\mathrm{d}x^4}\right) = q(x) \tag{42}$$

can be easily solved in the elastic range as a function of the ratio $\alpha = \ell/L$ together with the boundary conditions:

$$\begin{aligned} u(0) &= 0 \qquad \left.\frac{\mathrm{d}u}{\mathrm{d}x}\right|_{x=0} = 0 \\ u(L) &= \delta \qquad EA\left(\frac{\mathrm{d}^2u}{\mathrm{d}x^2}\right)_{x=L} = 0 \end{aligned} \tag{43}$$

Figure 4a shows the dimensionless axial displacement $u/L$ for an imposed displacement $\delta/L = 1$, as a function of the dimensionless abscissa $\xi = x/L$. The axial stress $\sigma/E$ and the hyperstress $\mu/EL$ plotted in Fig. 4b, c, are not constant along the bar, as are not the damage forces $\zeta_1/E$, $\zeta_2/E$, plotted in Fig. 4d, e. The driving force for the first gradient damage is maximum at the free end, while the opposite happens for $\zeta_2$, but both are of the same order of magnitude. It is important to point out that the second gradient damage force $\zeta_2$ presents a boundary layer near the built-in end, which becomes sharper and sharper as the internal length parameter $\alpha$ becomes small. The value of the activation function $g_d = (1-c)\,\zeta_1 + c\,\zeta_2$ divided by $E$ along the

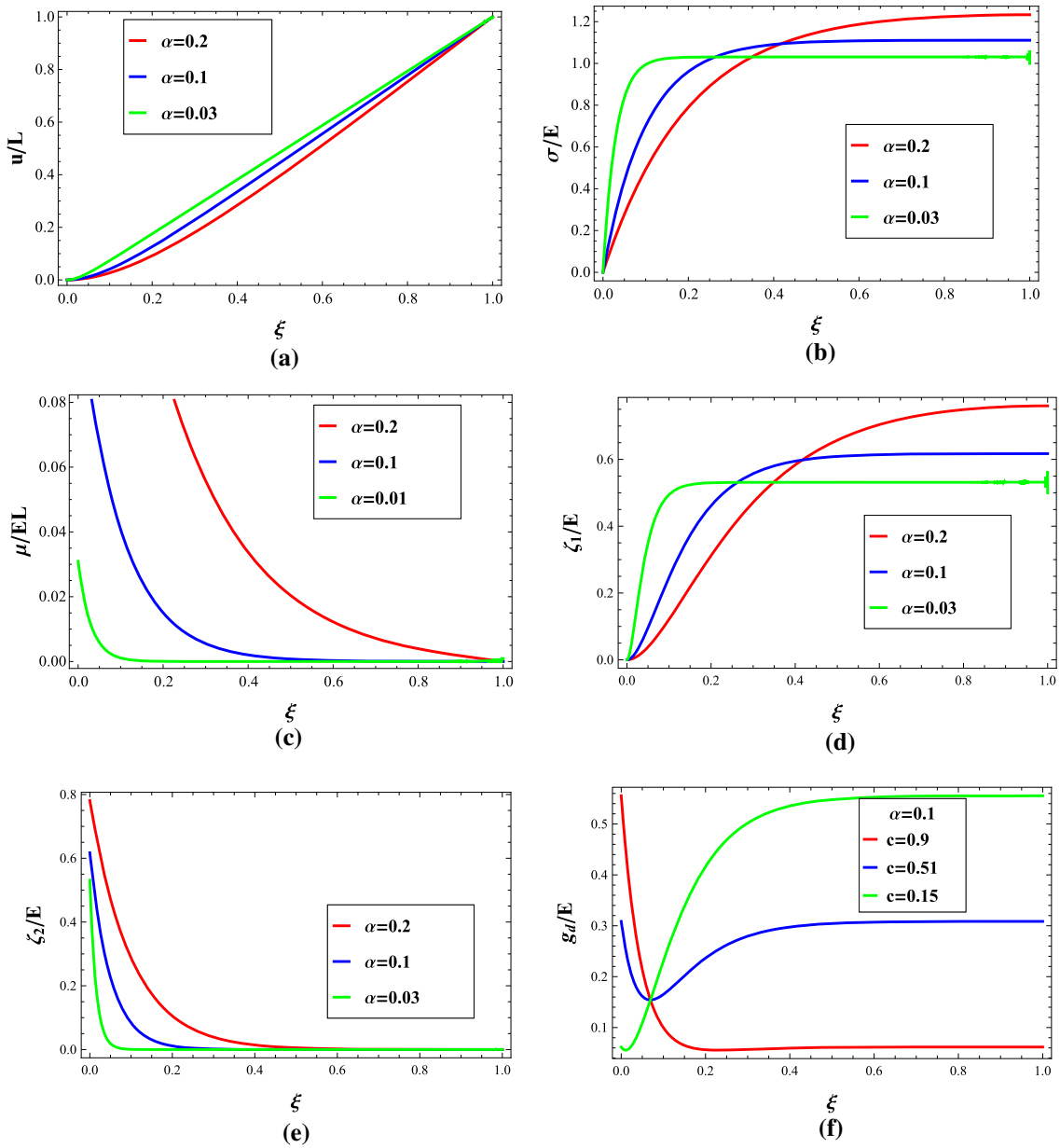


**Fig. 4** Uniaxial extension of an elastic bar. Second gradient model. Elastic solution. **a** Dimensionless axial displacement for various internal lengths. **b** Dimensionless stress $\frac{\sigma}{E} = \frac{\mathrm{d}u}{\mathrm{d}x}$. **c** Dimensionless hyperstress $\frac{\mu}{EL} = \alpha^2 \frac{\mathrm{d}^2 u}{\mathrm{d}x^2}$. **d** Dimensionless damage force $\frac{\zeta_1}{E} = \frac{n_1}{2}\left(\frac{\mathrm{d}u}{\mathrm{d}x}\right)^2$. **e** Dimensionless damage force $\frac{\zeta_2}{E} = \frac{n_2}{2}\alpha^2\left(\frac{\mathrm{d}^2 u}{\mathrm{d}x^2}\right)^2$. **f** Value of the activation function, as function of the weight $c$ for $\alpha = 0.1$

bar axis is shown for three values of the parameter $c$ in Fig. 4f. For $c < 0.5$ the maximum value of the activation function is reached at the free end, while for $c > 0.5$ the critical section becomes the built-in end. The two cases will be referred to as second gradient dominated ($c > 0.5$), and first gradient dominated ($c < 0.51$). In the balanced case $c = 0.5$ the same value of the activation function is reached at both ends of the bar, although $g_d$ is not constant along the axis. The activation function $g_d$ gets its largest value when $c = 0$ or $c = 1$, , while for the balanced case the activation function has the smallest value (Fig. 5).

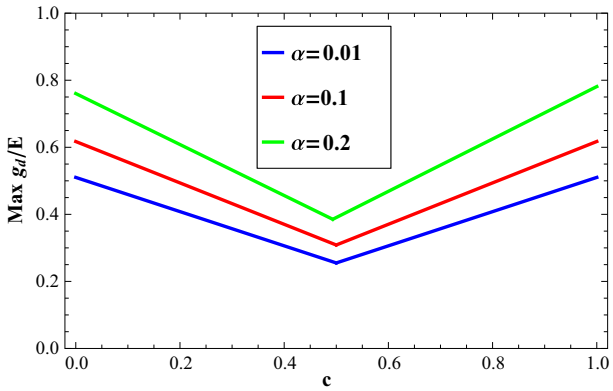


**Fig. 5** Uniaxial extension of an elastic bar. Second gradient model. Value of the activation function versus the parameter $c$

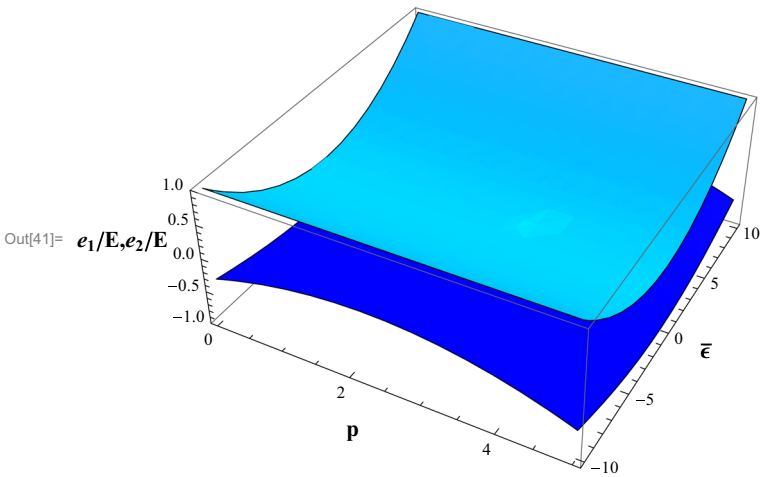


**Fig. 6** Uniaxial extension of an elastic bar. Strain gradient model. Eigenvalues of the tangent stiffness matrix. $n_1 = 2, n_2 = 2, \alpha = 0.1, c = 0.55$

The deformation in the part of the bar where the activation limit has been reached evolves according to the tangent stiffness, that, setting $\bar{\eta} = \eta L$, takes in the uniaxial case the following form:

$$
\begin{aligned}
&\begin{pmatrix} \frac{\dot{\sigma}}{E} \\ \frac{\dot{\mu}}{EL} \end{pmatrix} = \frac{1}{D_n} \begin{pmatrix} S_{11} & s_{12} \\ S_{12} & S_{22} \end{pmatrix} \begin{pmatrix} \dot{\varepsilon} \\ \dot{\eta} L \end{pmatrix} \\
&S_{11} = c^2 \frac{n_2}{2}(n_2 - 1)\alpha^2 \bar{\eta}_e^2 (1 + \omega_{1e})^{n_1} (1 + \omega_{2e})^{n_2 - 2} \\
&\qquad - (1 - c)^2 \frac{n_1}{2}(n_1 + 1)\varepsilon_e^2 (1 + \omega_{1e})^{2(n_1 - 1)} \\
&S_{12} = -c(1 - c)n_1 n_2 \alpha^2 \varepsilon_e \bar{\eta}_e (1 + \omega_{1e})^{n_1 - 1} (1 + \omega_{2e})^{n_2 - 1} \\
&S_{22} = (1 - c)^2 \frac{n_1}{2}(n_1 - 1)\alpha^2 \varepsilon_e^2 (1 + \omega_{1e})^{n_1 - 2} (1 + \omega_{2e})^{n_2} \\
&\qquad - c^2 \frac{n_2}{2}(n_2 + 1)\alpha^4 \bar{\eta}_e^2 (1 + \omega_{21e})^{2(n_2 - 1)} \\
&D_n = (1 - c)^2 \frac{n_1}{2}(n_1 - 1)\varepsilon_e^2 (1 + \omega_{1e})^{n_1 - 2} + c^2 \frac{n_2}{2}(n_2 - 1)\alpha^2 \bar{\eta}_e^2 (1 + \omega_{2e})^{n_2 - 2}
\end{aligned}
\tag{44}
$$

The matrix in (44) has one positive and one negative eigenvalue, for any value of the state variables, as can be easily checked from the signs of the determinant of the characteristic polynomial. Figure 6 shows for some choice of the constitutive parameters a plot of the eigenvalues of the constitutive tensor as a function of

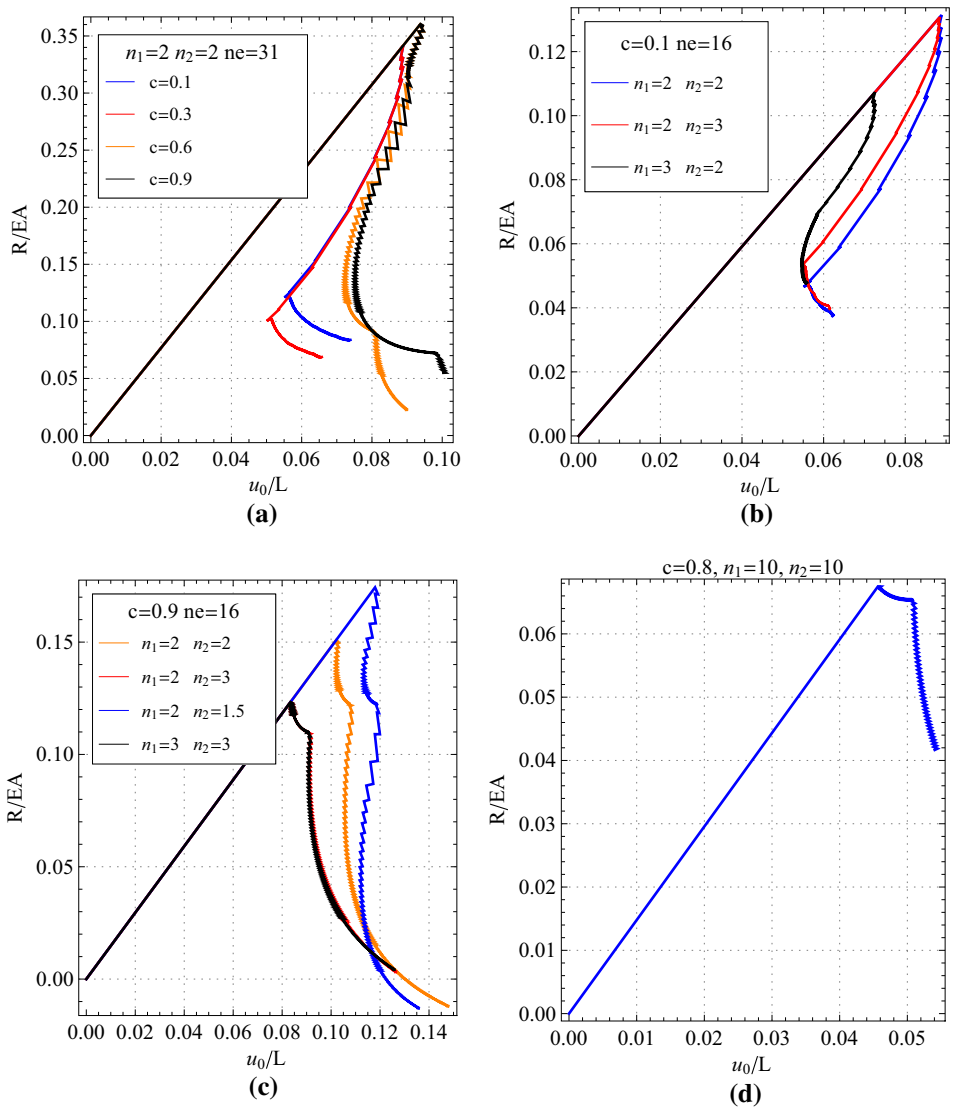


**Fig. 7** Uniaxial extension of a bar. Strain gradient model with damage. Dimensionless axial displacement versus end reaction. **a** Comparison of the results for different values of the parameter $c$. $n_1 = 2, n_2 = 2$, 31 elements. **b** First gradient-dominated material, $c = 0.1$, different $n_1, n_2$, 16 elements. **c** Second gradient-dominated material, $c = 0.9$, different $n_1, n_2$, 16 elements. **d** Second gradient-dominated material, $c = 0.8$, $n_1 = n_2 = 10$, 16 elements

the cumulated damage variable $p$ ($\omega_{1p} = (1 - c)\, p, \omega_{2p} = c\, p$) and of the ratio $\bar{\epsilon} = \frac{\eta_e L}{\varepsilon_e}$, from which it is possible to appreciate the difference of the sign of the two eigenvalues.

The positive definiteness of the tangent stiffness tensor in first gradient continua is a necessary condition for material stability. Strain localization then occurs when the acoustic tensor becomes singular for some direction, as happens in the case of damage. The situation is less clear in strain gradient continua. In [19] it was examined the case of softening plastic strain gradient materials. Also in that case the tangent stiffness tensors had coupling between first and second gradient terms, and both positive and negative eigenvalues, but no localization occurred, similarly to the classical models of gradient plasticity [52]. The question will now be discussed with reference to the uniaxial damage example presented. Given the highly nonlinear nature of the equations, the problem will be solved numerically.

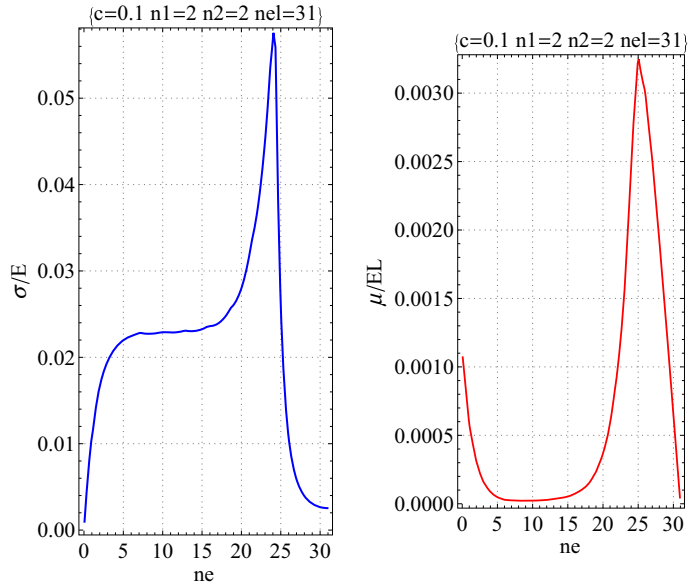


**Fig. 8** Uniaxial extension of an elastic bar. Strain gradient model with damage. $c = 0.1n_1 = 2n_2 = 2$. Distribution of stress $\sigma_{11}/E$ and hyperstress $\mu_{111}/EL$ along the bar

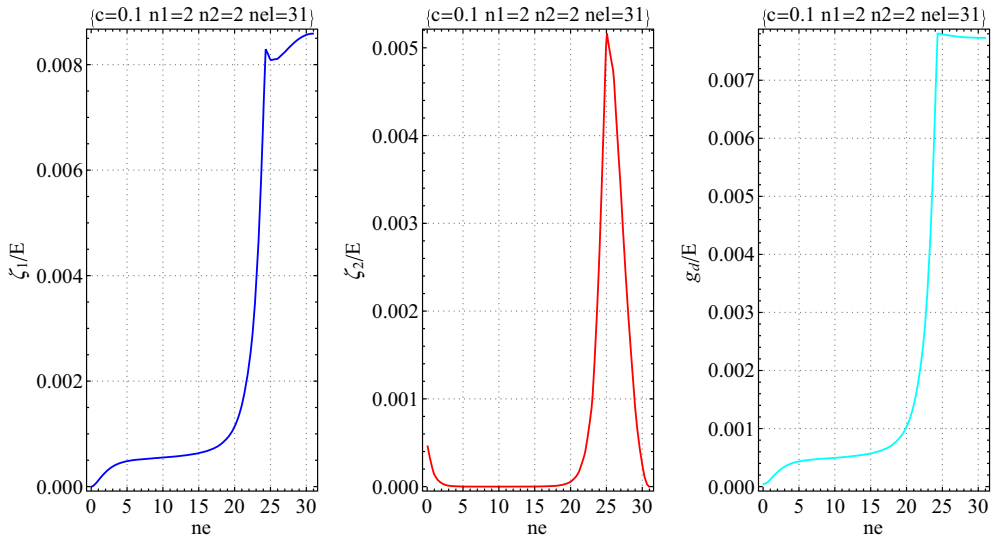


**Fig. 9** Uniaxial extension of an elastic bar. Strain gradient model with damage. $c = 0.1n_1 = 2n_2 = 2$. Distribution of the damage forces $\zeta_1/E$, $\zeta_2/E$ and of the activation function $g_d/E$ along the bar

## 4.1 Numerical simulations

$C^1$ continuity is required for strain gradient materials; in addition, since large discontinuities can occur on the strain gradient once damage develops, it is desirable that also the second derivatives present some degree of regularity. Therefore a B-spline approximation has been used. Isogeometric analysis is largely diffused for polar structural models [12,42,43,47], and presents many desirable properties of stability and accuracy. The bar is modelled with a single patch, and cubic splines are used, with an open knot vector having $n$ distinct internal points, corresponding to $n + 1$ elements. Refinement is obtained by knot insertion. In this way second degree continuity is obtained between elements.

The damage response of the bar is characterized by a sharp snap back, like in the case of first gradient models. For fixed values of the damage exponents $n_1$, $n_2$ the post-peak response differs between first gradient- and second gradient-dominated models, the latter presenting a less severe snap back (Fig. 7a). For first gradient-

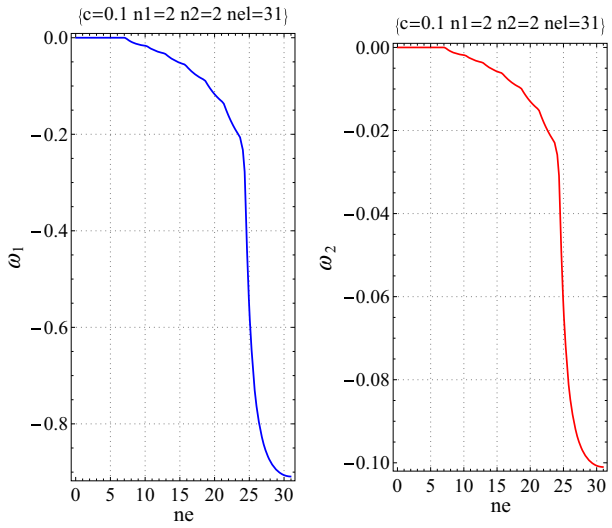


**Fig. 10** Uniaxial extension of an elastic bar. Strain gradient model with damage. $c = 0.1n_1 = 2n_2 = 2$. Cumulated damage $\omega_{1e}, \omega_{2e}$ along the bar at the end of the simulation

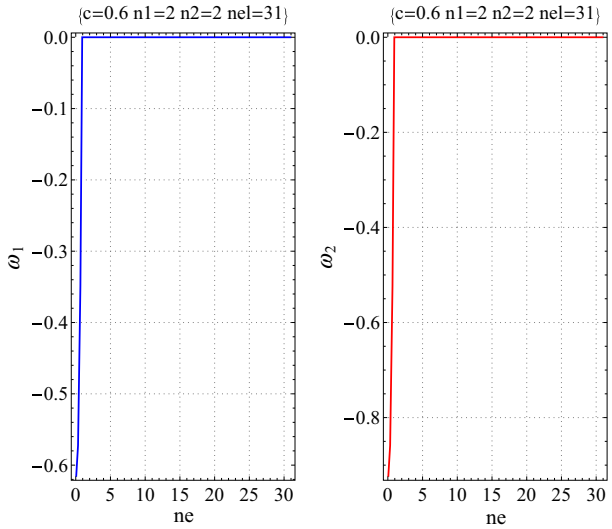


**Fig. 11** Uniaxial extension of an elastic bar. Strain gradient model with damage. $c = 0.1n_1 = 2n_2 = 2$. Cumulated damage $\omega_{1e}, \omega_{2e}$ along the bar at the end of the simulation

dominated models ($c = 0.1$, see Fig. 7b), the value of the exponent $n_1$ largely affects the result, while it is almost insensitive to the value of the exponent of the second gradient damage $n_2$. The opposite happens for second gradient-dominated models ($c = 0.9$, Fig. 7c). For larger values of $n_2$ snap back does not occur, a result that is not found with first gradient damage-dominated materials. This is shown in Fig. 7d, that refers to the case $c = 0.8$, with very large values of the damage exponents.

A better insight can be obtained analysing the distribution of the internal forces and of the cumulated damage within the bar. They are represented in the following figures against the element number, ne. For small values of the parameter $c$ damage initiates at the free end of the bar; as a consequence, in the damaged zone the stress and the hyperstress decrease, Fig. 8, corresponding to an almost constant value of $\zeta_1$, while $\zeta_2$ is close to zero. Both damage forces grow to large values ahead of the damaged zone, Fig. 9. The cumulated damage internal variables start to grow from the free end and then spread over almost the whole bar ate the end of the simulation, corresponding to the annihilation of the strength of the material (Fig. 10).

In the case $c > 0.5$, on the contrary, damage starts at the first extremity of the bar and appears to localize without spreading along the beam (Fig. 11). Due to the presence of large strain gradients (Fig. 12), the damage

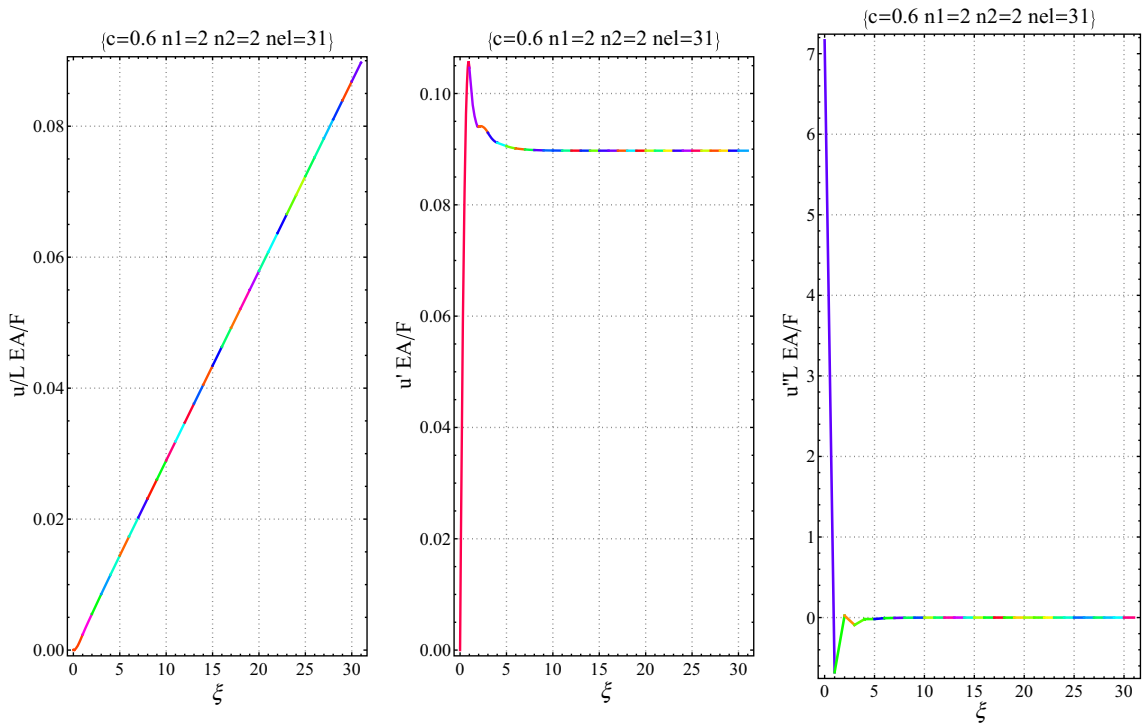


**Fig. 12** Uniaxial extension of an elastic bar. Strain gradient model with damage. $c = 0.6 n_1 = 2 n_2 = 2$. Displacement, first and second gradients of displacement along the bar

force $\zeta_2$ presents a very sharp boundary layer (Fig. 13), that induces localization (the spikes present in the load displacement curves of Fig. 7c, relative to the case $c = 0.9, n_1 = 2, n_2 = 2$, correspond to the activation of subsequent Gauss points, and it can be seen that just a few of them are interested by damage before the axial force reduces to zero). The solution found is nearly the same for all the discretizations that have been tried, provided the first Gauss point is located at the extremity of the beam (Gauss-Lobatto integration had to be used).

## 5 Conclusions

A continuum damage model for non-local materials has been proposed. The model has been presented for strain gradient materials, coupled with elasto-plasticity. A particularization to the case of pure damage has been studied with some more details with the aid of an uniaxial example. The main point of the model is that two separate damage variables, affecting first and second gradient stiffness, have been introduced, that evolve independently according to their own evolution law. That is, the damage internal variable for the second gradient stiffness is not the gradient of the damage variable for the first gradient stiffness. Therefore there is no need of additional field equations, and the damage variable can be obtained locally by the constitutive equations. The model has been set within a thermodynamic consistent framework, defined by means of the internal energy potential and the dissipation functional, according to the Generalized Standard Material Model.

In the paper only the case of scalar damage has been studied. The more realistic case of anisotropic damage for higher gradient materials still requires further analysis. The anelastic tangent stiffness operator presents coupling between first and second gradient terms, even though the elastic constitutive tensors had been chosen uncoupled. In the uniaxial case, it has been shown that the tangent stiffness tensor has one positive eigenvalue and one negative eigenvalue, contrarily to the case of the first gradient continuum damage material.

With the aid of an uniaxial example of the extension of a non-local bar, it has been found that for first-gradient-damage-dominated materials the damage variables diffuse over the domain, that is, the strain localization phenomena occurring in local damage, that makes the model useless per se for numerical simulations, is not present. For second gradient-dominated materials from the simulations performed localization of damage still appears to occur, but that is due to a sharp boundary layer present in the elastic solution. The matter,

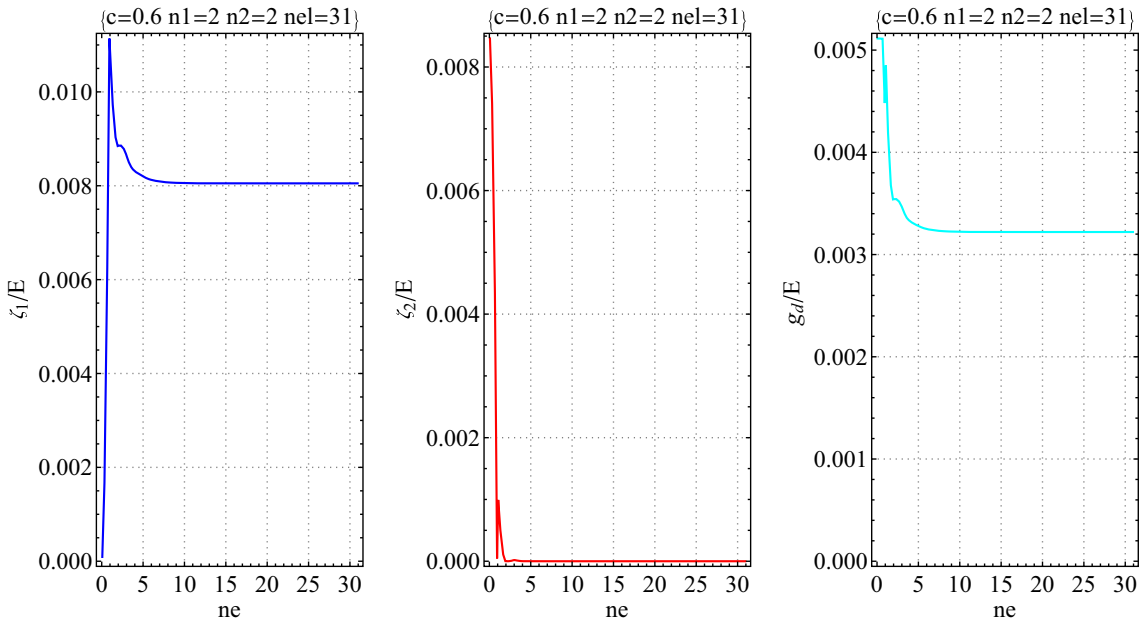


**Fig. 13** Uniaxial extension of an elastic bar. Strain gradient model with damage. $c = 0.6n_1 = 2n_2 = 2$. Distribution of the damage forces $\zeta_1/E$, $\zeta_2/E$ and of the activation function $g_d/E$ along the bar at the end of the simulation

however, deserves further analysis with the aid of more general models and simulations and will be object of future developments.

## References


1. Addessi, D., Sacco, E., Paolone, A.: Cosserat model for periodic masonry deduced by nonlinear homogenization. Eur. J. Mech. A. Solids **29**(4), 724–737 (2010)
2. Aifantis, E.: On the gradient approach relation to eringens nonlocal theory. Int. J. Eng. Sci. **49**, 1367–1377 (2011)
3. Aifantis, E.: Update on a class of gradient theories. Mech. Mater. **35**, 259–280 (2013)
4. Aifantis, K., Konstantinidis, A., Forest, S.: Modeling strain localization bands in metal foams. J. Comput. Theor. Nanosci. **7**, 1–7 (2010)
5. Alibert, J.J., Seppecher, P., dell' Isola, F.: Truss modular beams with deformation energy depending on higher displacement gradients. Math. Mech. Solids **8**(1), 51–73 (2003)
6. Altenbach, H., Eremeyev, V.: On the bending of viscoelastic plates made of polymer foams. Acta Mech. **204**, 137–154 (2009)
7. Altenbach, H., Eremeyev, V., Lebedev, L., Rendón, L.: Acceleration waves and ellipticity in thermoelastic micropolar media. Arch. Appl. Mech. **80**(3), 217–227 (2010)
8. Arabnejad, S., Pasini, G.: Mechanical properties of lattice materials via asymptotic homogenization and comparison with alternative homogenization methods. Int. J. Mech. Sci. **77**(4), 249–262 (2013)
9. Baravelli, E., Ruzzene, M.: Internally resonating lattices for bandgap generation and low-frequency vibration control. J. Sound Vib. **332**(25), 6562–6579 (2013)
10. Bertram, A.: Finite gradient elasticity and plasticity: a constitutive mechanical framework. Continuum Mech. Thermodyn. **27**, 1039–1058 (2015)
11. Bigoni, D., Loret, B., Radi, E.: Localization of deformation in plane elastic–plastic solids with anisotropic elasticity. J. Mech. Phys. Solids **48**, 1441–1466 (2000)
12. Borden, M.J., Scott, M.A., Evans, K.A., Hughes, T.J.R.: Isogeometric finite element data structures based on Bezier extraction of NURBS. Int. J. Numer. Methods Eng. **87**, 15–47 (2011)
13. Boutin, C.: Behavior of poroelastic isotropic beam derivation by asymptotic expansion method. J. Mech. Phys. Solids **60**(6), 1063–1087 (2012)
14. Boutin, C., dell Isola, F., Giorgio, I., Placidi, L.: Linear pantographic sheets: asymptotic micro-macro models identification. Math. Mech. Complex Syst. **5**(2), 127–162 (2017)
15. Braides, A., Garroni, A.: Homogenization of periodic nonlinear media with stiff and soft inclusions. Math. Models Methods Appl. Sci **05**(4), 543–564 (1995)
16. Contrafatto, L., Cuomo, M.: A new thermodynamically consistent continuum model for hardening plasticity coupled with damage. Int. J. Solids Struct. **39**, 6241–6271 (2002)

17. Covezzi, F., de Miranda, S., Marfia, S., Sacco, E.: Complementary formulation of the tfa for the elasto-plastic analysis of composites. Compos. Struct. **156**, 93–100 (2016)
18. Cuomo, M., Dell Isola, F., Greco, L., Rizzi, N.L.: First versus second gradient energies for planar sheets with two families of inextensible fibres: investigation on deformation boundary layers, discontinuities and geometrical instabilities. Compos. Part B Eng. https://doi.org/10.1016/j.compositesb.2016.08.043 (2016)
19. Cuomo, M.: Continuum model of microstructure induced softening for strain gradient materials. Math. Mech. Solids accepted (2018)
20. Cuomo, M.: Forms of the dissipation function for a class of viscoplastic models. Math. Mech. Complex Syst. **5**(3), 217–237 (2017)
21. Cuomo, M., Fagone, M.: Finite deformation non-isotropic elasto-plasticity with evolving structural tensors: a framework. Il Nuovo Cimento **32**(1), 55–72 (2009)
22. Cuomo, M., Fagone, M.: Model of anisotropic elastoplasticity in finite deformations allowing for the evolution of the symmetry group. Nanomech. Sci. Technol.: Int. J. **6**(2), 135–160 (2015)
23. De Felice, G., Amorosi, A., Malena, M.: Elasto-plastic analysis of block structures through a homogenization method. Int. J. Numer. Anal. Meth. Geomech. **34**, 221–247 (2009)
24. Dell Isola, F., Giorgio, I., Pawlikowski, M., Rizzi, N.L.: Large deformations of planar extensible beams and pantographic lattices: heuristic homogenization, experimental and numerical examples of equilibrium. Proc. R. Soc. Lond. A **472**(2185), 20150790 (2016)
25. Dell Isola, F., Steigmann, D., Della Corte, A.: Synthesis of fibrous complex structures: designing microstructure to deliver targeted macroscale response. Appl. Mech. Rev. **67**(6), 060804 (2016)
26. Deshpande, V., Fleck, N.: Isotropic constitutive models for metallic foams. J. Mech. Phys. Solids **48**, 1253–1283 (2000)
27. Dietsche, A., Steinmann, P., Willam, K.: Micropolar elastoplasticity and its role in localization. Int. J. Plast. **9**(7), 813–831 (1993)
28. Eremeyev, V., Lebedev, L., Cloud, M.: Acceleration waves in the nonlinear micromorphic continuum. Mech. Res. Commun. https://doi.org/10.1016/j.mechrescom.2017.07.004 (2017)
29. Eu, B.: Nonequiibrium Statistical Mechanics: Ensemble Method. Kluwer, Dordrecht (1998)
30. Fleck, N., Hutchinson, J.: A reformulation of strain gradient plasticity. J. Mech. Phys. Solids **49**, 2245–2271 (2001)
31. Forest, S.: Micromorphic approach for gradient elasticity, viscoplasticity, and damage. J. Eng. Mech. ASCE **135**(3), 117–131 (2009)
32. Forest, S.: Nonlinear regularization operators as derived from the micromorphic approach to gradient plasticity. Proc. R. Soc. A **472**, 20150755 (2016)
33. Forest, S., Aifantis, E.: Some links between recent gradient thermoelastoplasticity theories and the thermomechanics of generalized continua. Int. J. Solids Struct. **47**, 3367–3376 (2010)
34. Forest, S., Blazy, J.S., Chastel, Y., Moussy, F.: Continuum modeling of strain localization phenomena in metallic foams. J. Mater. Sci. **40**, 5903–5910 (2005)
35. Gaitanaros, S., Kyriakides, S.: Dynamic crushing of aluminum foams: Part I experiments. Int. J. Solids Struct. **51**, 1631–1645 (2014)
36. Ganghoffer, J., Sluys, L., de Borst, R.: A reappraisal of nonlocal mechanics. Eur. J. Mech. A/Solids **18**, 17–46 (1999)
37. Ghiba, I.D., Neff, P., Madeo, A., Placidi, L., Rosi, G.: The relaxed linear micromorphic continuum: existence, uniqueness and continuous dependence in dynamics. Math. Mech. Solids **20**(10), 1171–1197 (2015)
38. Goda, I., Assidi, M., Ganghoffer, J.F.: Equivalent mechanical properties of textile monolayers from discrete asymptotic homogenization. J. Mech. Phys. Solids **61**, 2537–2565 (2013)
39. Goddard, J.: Edelens dissipation potentials and the visco-plasticity of particulate media. Acta Mech. **225**, 2239–2259 (2014)
40. Gorlach, M., Voytova, T., Lapine, M., Kivshar, Y., Belov, P.: Nonlocal homogenization for nonlinear metamaterials. Phys. Rev. B **93**, 165125 (2016)
41. Grammenoudis, F., Tsakmakis, C., Hofer, D.: Micromorphic continuum. Part III: small deformation plasticity coupled with damage. Int. J. Non-Linear Mech. **45**(2), 140–148 (2010)
42. Greco, L., Cuomo, M.: An implicit $g^1$ multi patch b-spline interpolation for kirchhoff-love space rod
43. Greco, L., Cuomo, M.: An isogeometric implicit $g^1$ mixed finite element for kirchhoff space rods. Comput. Methods Appl. Mech. Eng. **298**, 325–349 (2016)
44. Halphen, B., Nguyen, Q.: Sur les matériaux standards généralisés. J. de Mec. **14**, 3963 (1975)
45. Iltchev, A., Marcadon, V., Kruch, S., Forest, S.: Computational homogenisation of periodic cellular materials: application to structural modelling. Int. J. Mech. Sci. **93**, 240–255 (2015)
46. Jiràsek, M., Rokos, O., Zeman, J.: Localization analysis of variationally based gradient plasticity model. Int. J. Solids Struct. **50**, 256–269 (2013)
47. Kiendl, J., Bletzinger, K., Linhard, J., Wuchner, R.: Isogeometric shell analysis with Kirchhoff–Love elements. Comput. Methods Appl. Mech. Eng. **198**, 3902–3914 (2009)
48. Lemaitre, J., Desmorat, R.: Engineering Damage Mechanics : Ductile, Creep, Fatigue and Brittle Failures. Springer, Berlin (2005)
49. Marfia, S., Sacco, E.: Computational homogenization of composites experiencing plasticity, cracking and debonding phenomena. Comput. Methods Appl. Mech. Eng. **304**, 319342 (2016)
50. Miehe, C.: Variational gradient plasticity at finite strains. Part I: mixed potentials for the evolution and update problems of gradient-extended dissipative solids. Comput. Methods Appl. Mech. Eng. **268**, 677–703 (2014)
51. Misra, A., Placidi, L., Scerrato, D.: A review of presentations and discussions of the workshop computational mechanics of generalized continua and applications to materials with microstructure that was held in catania 29–31/10/2015. Math. Mech. Solids **22**, 1891–1904 (2017)
52. Ning, J., Aifantis, E.: Gradient theory and its applications to stability analysis of materials and structures. J. Mech. Behav. Mater. **7**(4), 235–263 (1996)
53. Olurin, O., Fleck, N., Ashby, M.: Deformation and fracture of aluminium foams. Mater. Sci. Eng. A **291**, 136–146 (2000)

54. Placidi, L.: A variational approach for a nonlinear 1-dimensional second gradient continuum damage model. Continuum Mech. Thermodyn. **27**, 623–638 (2015)
55. Placidi, L.: A variational approach for a nonlinear one-dimensional damage-elasto-plastic second gradient continuum model. Continuum Mech. Thermodyn. **28**(1–2), 119–137 (2016)
56. Placidi, L., Barchiesi, E., Turco, E., Rizzi, N.: A review on 2d models for the description of pantographic fabrics. Z. Angew. Math. Phys. **67**, 1–20 (2016)
57. Placidi, L., Giorgio, I., Della Corte, A., Scerrato, D.: Generalized continua and their applications to the design of composites and metamaterials: a review of presentations and discussions. Math. Mech. Solids **22**, 1–14 (2017)
58. Rahali, Y., Giorgio, I., Ganghoffer, J., dell Isola, F.: Homogenization la piola produces second gradient continuum models for linear pantographic lattices. Int. J. Eng. Sci. **97**, 148–172 (2015)
59. Regueiro, R.: On finite strain micromorphic elastoplasticity. Int. J. Solids Struct. **47**, 786–800 (2010)
60. Rinaldi, A., Placidi, L.: A microscale second gradient approximation of the damage parameter of quasi-brittle heterogeneous lattices. ZAMM **94**(102), 862–877 (2014)
61. Saanouni, K., Hamed, M.: Micromorphic approach for finite gradient-elastoplasticity fully coupled with ductile damage: formulation and computational aspects. Int. J. Solids Struct. **50**, 22892309 (2013)
62. San Marchi, C., Despois, J.F., Mortensen, A.: Uniaxial deformation of open-cell aluminum foam: the role of internal damage. Acta Mater. **52**, 2895–2902 (2004)
63. Seppecher, P., Alibert, J.J., dell' Isola, F.: Linear elastic trusses leading to continua with exotic mechanical interactions. J. Phys. Conf. Ser. **319**(1) (2011)
64. Sluys, L.: Wave propagation and localization in a rate-dependent cracked medium—model formulation and one-dimensional example. Int. J. Solids Struct. **29**, 2945–2958 (1992)
65. Tollenaere, H., Cailleri, D.: Continuous modeling of lattice structures by homogenization. Adv. Eng. Softw. **29**(7–9), 699–705 (1998)
66. Turco, E., dell Isola, F., Cazzani, A., Rizzi, N.L.: Hencky-type discrete model for pantographic structures: numerical comparison with second gradient continuum models. Zeitschrift fr Angewandte Math. und Phys. **67**(4), 85 (2016)
67. Vardoulakis, I.: Potentials and limitations of softening models in geomechenics. Eur. J. Mech. A/Solids **13**, 195–226 (1994)
68. Vardoulakis, I., Aifantis, E.: A gradient flow theory of plasticity for granular materials. Acta Mech. **87**, 197–217 (1991)
69. Velasco, R., Scherer García-Colín, L., Uribe, F.: Entropy production: its role in non-equilibrium thermodynamics. Entropy **13**, 82–116 (2011)
70. Zaiser, M., Aifantis, E.: Avalanches and slip patterning in plastic deformation. J. Mech. Behav. Mater. **14**(4–5), 255–270 (2003)